

# Novel detection of aerosols: combined cavity ring-down and fluorescence spectroscopy

Bruce A. Richman, Alexander A. Kachanov, and Barbara A. Paldus

*Picarro, Inc., 480 Oakmead Parkway, Sunnyvale, CA 94085*

[brichman@picarro.com](mailto:brichman@picarro.com), [akachanov@picarro.com](mailto:akachanov@picarro.com), [bpaldus@picarro.com](mailto:bpaldus@picarro.com)

Anthony W. Strawa

*NASA-Ames Research Center, Mail Stop 245-4, Moffett Field, CA 94035*

[astrawa@mail.arc.nasa.gov](mailto:astrawa@mail.arc.nasa.gov)

**Abstract:** High fluences inside cavity ring-down spectroscopy optical resonators lend themselves to fluorescence or nonlinear optical spectroscopy. An instrument at 488 nm was developed to measure extinction, and fluorescence of aerosols. A detection limit of  $6 \times 10^{-9} \text{ cm}^{-1} \text{ Hz}^{-1/2}$  ( $0.6 \text{ Mm}^{-1} \text{ Hz}^{-1/2}$ ) was achieved. The fluorescence spectral power collected from a single fluorescent microsphere was 10 to 20 pW/nm. This power is sufficient to obtain the spectrum of a single microsphere with a resolution of 10 nm and signal-to-noise ratio of  $\sim 10$ . The relative concentrations of two types of fluorescent microspheres were determined from a time-integrated fluorescence measurement of a mixture of both.

©2005 Optical Society of America

OCIS codes: (300.6360) Spectroscopy, laser; (300.2530) Fluorescence, laser induced.

---

## References and links

1. Y. Pan, S. Holler, et al., "Single-shot fluorescence spectra of individual micrometer-sized bioaerosols illuminated by a 351- or a 266-nm ultraviolet laser," *Opt. Lett.* **24**, 116-118 (1999).
2. Y.-L. Pan, J. Hartings, R. G. Pinnick, S. C. Hill, J. Halverson, and R. K. Chang, "Single-Particle Fluorescence Spectrometer for Ambient Aerosols," *Aer. Science and Tech.* **37**, 627-638 (2003).
3. F. L. Reyes, T. H. Jeys, et al., "Bio-aerosol fluorescence sensor," *Field Anal. Chem. and Tech.* **3**, 240-248 (1999).
4. Y.-L. Pan, V. Boutou, R. K. Chang, I. Ozden, K. Davitt, and A. V. Nurmikko, "Application of light-emitting diodes for aerosol fluorescence detection," *Optics Letters* **28**, 1707-1709 (2003).
5. J. J. L. Spaanjaars, J. J. t. Meulen, and G. Meijer, "Relative predissociation rates of OH ( $A^2\Sigma^+$ ,  $v'=3$ ) from combined cavity ring down—Laser-induced fluorescence measurements," *Journal of Chemical Physics* **107**, 2242-2248 (1997).
6. J. Luque, J. B. Jeffries, G. P. Smith, D. R. Crosley, and J. J. Scherer, "Combined cavity ringdown absorption and laser-induced fluorescence imaging measurements of CN(B-X) and CH(B-X) in low-pressure  $\text{CH}_4\text{-O}_2\text{-N}_2$  and  $\text{CH}_4\text{-NO-O}_2\text{-N}_2$  flames," *Combustion and Flame* **126**, 1725-1735 (2001).
7. A. W. Strawa, R. Casteneda, et al., "The Measurements of Aerosol Optical Properties using Continuous Wave Cavity Ring-down Techniques," *J. Atmos. And Ocean Tech.* **20**, 454-465 (2003).
8. A. D. Sappey, E. S. Hill, et al. "Fixed-frequency cavity ringdown diagnostic for atmospheric particulate matter," *Opt. Lett.* **23**, 954-956 (1998).
9. R. L. VanderWal and T. M. Ticich, "Cavity ringdown and laser-induced incandescence measurements of soot," *Appl. Opt.* **38**, 1444-1451 (1999).
10. J. D. Smith and D. B. Atkinson, "A portable pulsed cavity ring-down transmissometer for measurement of the optical extinction of the atmospheric aerosol," *Analyst* **126**, 1216-1220 (2001).
11. V. Bulatov, M. Fisher, and I. Schechter, "Aerosol Analysis by cavity-ring-down spectroscopy," *Anal. Chim. Acta* **466**, 1-9 (2002).
12. Pettersson, A., E. R. Lovejoy, et al. "Measurement of aerosol optical extinction at 532 nm with pulsed cavity ring-down spectroscopy," *J. Aerosol Sci.* **35**, 995-1011(2004).
13. H. Mossmuller, R. Varma, et al.. "Cavity Ring-down and Cavity-Enhanced Detection Techniques for the Measurement for Aerosol Extinction," *Aerosol Sci. Tech.* **39**, 30-39(2005).

14. B. A. Paldus, R. Provencal, and A. Kachanov, "Cavity Enhanced Optical Detector," U.S. Patent Application 10/738,599 (2004).
  15. K. W. Busch and M. A. Busch (Eds.), "Cavity ring-down spectroscopy: An ultratrace absorption measurement technique," ACS Symp. Ser **720** (1999).
  16. J. Morville, D. Romanini, M. Chenevier, and A. Kachanov, "Effects of laser phase noise on the injection of a high-finesse cavity", Appl. Opt. **41**, 6980-6990 (2002).
  17. K. L. Bechtel, R. N. Zare, et al., "Moving Beyond Traditional UV-Vis Absorption Detection: Cavity Ring-Down Spectroscopy for HPLC," Anal. Chem. **77**, 1177-1182 (2005).
- 

## 1. Introduction

Bioaerosols are airborne particles from living organisms such as bacteria, viruses, molds, fungi, pollens, dust mite or insect remains, and pet dander. They have both natural and anthropogenic sources and are ubiquitous in the earth's tropospheric boundary layer. While most atmospheric bioaerosols are harmless, some bioaerosols can cause disease, allergies, and respiratory problems. There is a need to quantify airborne microorganisms for the biotechnology industry, the evaluation of indoor air quality, investigations of infectious disease outbreaks, and agricultural health investigations. To determine the sources and effects of bioaerosols on human and animal health, a need exists for an instrument that is capable of accurately and reliably measuring aerosol optical properties while simultaneously discriminating between biological and non-biological aerosols.

Real-time methods for the detection and identification of atmospheric particles remain limited in capability. Polymerase chain reaction (PCR) based cytometry methods for biological particle identification require too much time for sample amplification and analysis. Most existing methods to detect and characterize aerosols require the collection of samples on a filter over a period of several minutes, and measuring the change in filter transmission. However, the absorption coefficient is usually small, hence real-time, *in situ* monitoring is impractical.

A need therefore exists to develop methods which can concurrently characterize the physical characteristics of an aerosol and identify the particulates that comprise it. Experiments that obtained fluorescence emission spectra for several aerosols have illustrated that it might be possible to discriminate between biological and non-biological aerosols using this approach. For example, Pan *et al.* [1, 2] showed the contrast between bacterial spores and particles from non-biological aerosols such as carbon black by measuring their fluorescence emission after excitation with 266 nm light [3]. UV light generation at high power levels results in laser designs that consume high power, are very expensive (>\$50,000), or are bulky (e.g. pulsed Nd:YAG lasers), limiting the practical deployment of this technology into field applications. More recent research from the same group [4] used an array of LEDs instead of a high power laser to effect the fluorescence excitation. Another method to obtain effectively high excitation power is to use high finesse build-up cavities, such as those used in cavity ring-down spectroscopy (CRDS), with lower power, small, lightweight continuous wave (CW) UV lasers. Moreover, the fluorescence measurement can be combined with CRDS and scattering measurements, as well as multiple excitation wavelengths, to fully characterize the aerosol. CRDS offers high sensitivity to optical losses, and can be used to detect the presence of individual aerosol particles. The combination of fluorescence and CRDS was demonstrated on chemical components of a flame by Spaanjaars *et al* [5], and also by Luque *et al* [6].

Picarro and NASA Ames Research Center successfully developed a first-generation CRDS optical analyzer (*Cadenza II*) for real-time determination of aerosol optical properties *in-situ* [7] using continuous wave (CW) lasers. The presence of aerosol particles increases the cavity's decay rate, owing to scattering and absorption. By measuring the decay rate of the cavity, a CRDS instrument can determine the extinction of the aerosols with extreme sensitivity. *Cadenza II* could measure optical extinction at both 675 and 1550 nm and scattering at 675 nm.

Previous efforts to measure aerosol extinction with CRDS primarily used pulsed lasers. Sappey *et al* [8] used a pulsed Nd-YAG laser source at 532 and 355 nm wavelength in a one meter cell to measure an extinction coefficient of  $2 \times 10^{-7} \text{ m}^{-1}$  ( $0.2 \text{ Mm}^{-1}$ ). They compared the

sensitivity of their system to that of a Met One Model 237H laser particle counter that uses light scattering to detect individual aerosol particles. Van der Wal and Ticich [9] also used a pulsed system to measure soot volume fraction in flames. They were able to measure an extinction coefficient of  $400 \text{ Mm}^{-1}$  in a 1 cm sooting flame. More recently, Smith and Atkinson [10] used a pulsed CRD system with a Nd-YAG laser to measure aerosol extinction at wavelengths of 532 and 1064 nm in a one meter cell. This system was similar to that of Sappey et al. and recorded an extinction of about  $50 \text{ Mm}^{-1}$  at a wavelength of 532 nm. A similar system using a pulsed dye laser was developed by Bulatov *et al.* [11] and achieved a detection limit of  $8 \text{ Mm}^{-1}$  at a wavelength of 620 nm. This system was used to investigate the properties of NaCl and  $\text{CuCl}_2 \cdot 2\text{H}_2\text{O}$  aerosols. More recent experiments on aerosols using pulsed Nd:YAG lasers were made by Pettersson [12] in 2004 and Mossmuller [13] in 2005.

The CW-CRDS aerosol work demonstrated that by using CW lasers, high optical intensities could build up within the ring-down cavity. It was realized that such high intracavity fluences could enhance the detectable fluorescence signals from the aerosols, or lead to non-linear processes such as stimulated Raman scattering [14]. This paper presents the first concurrent measurements of absorption, scattering and fluorescence of aerosols using CRDS and a low power, CW laser source. The work was carried out at 488 nm, because single-mode, narrow linewidth CW lasers in the UV ( $< 300 \text{ nm}$ ) are currently unavailable, and synthetic fluorophores for generating test aerosols are readily available.

## 2. Cavity ring-down spectroscopy combined with fluorescence

### 2.1 Cavity ring-down spectroscopy

Cavity ring-down spectroscopy (CRDS) is based on the principle of measuring the rate of decay of light intensity inside a high finesse optical resonator called the ring-down cavity (RDC). The transmitted wave decays exponentially in time. The decay rate is proportional to the total optical losses inside the RDC. In a typical CRDS setup, light from a laser is first injected into the RDC, and is then interrupted. The circulating light inside the RDC is both scattered and transmitted by the mirrors on every round-trip, and can be monitored using a photodetector placed behind one of the cavity mirrors. The decay constant, also called the ring-down time,  $\tau$ , is then measured as a function of laser wavelength to obtain a spectrum of the cavity optical losses. Detailed mathematical treatments of CRDS can be found in [15]. For a given wavelength,  $\lambda$ , the transmitted light,  $I(t, \lambda)$ , from the RDC is given by,

$$I(t, \lambda) = I_0 e^{-t/\tau(\lambda)} \quad (1)$$

where  $I_0$  is the transmitted light at the time the light source is shut off, and  $\tau(\lambda)$  is the ring-down time constant. The optical loss inside the cavity expressed in units of an absorption coefficient ( $\text{cm}^{-1}$ ) is  $L(\lambda) = [c\tau(\lambda)]^{-1}$ , where  $c$  is the speed of light. The total optical loss comprises the empty cavity optical loss and the sample optical loss. CRDS provides an absolute measurement of these optical losses. The empty cavity (round-trip) optical loss,  $L_{\text{empty}}(\lambda)$ , comprises the scattering and transmission losses of the mirrors. In general, better mirrors provide lower empty cavity losses and higher sensitivity.

In the present approach, the extinction coefficient is given by the difference between measurements made when the cell contains filtered air and when the cell contains a particulate-laden flow:

$$\sigma_{\text{ext}} = \frac{1}{c} \left( \frac{1}{\tau_{\text{aer}}} - \frac{1}{\tau_0} \right) \quad (2)$$

where  $\tau_{\text{aer}}$  is the ring-down time of the aerosol laden flow and  $\tau_0$  is for the filtered air.

The minimum detectable absorption loss (MDAL) for a CRDS system is defined by,

$$\alpha_{\text{min}} = \frac{1}{l_{\text{eff}}} \left( \frac{\Delta\tau}{\tau} \right), \quad (3)$$

where  $\Delta\tau/\tau$  is the ring-down-to-ring-down (shot-to-shot) noise of the system. The effective path length of a CRDS measurement is  $l_{\text{eff}} = c\tau_0$ . For typical RDC mirrors having a reflectivity of 99.995%, and scattering losses of less than 0.0005%, the path length enhancement,  $l_{\text{eff}}/l_{\text{cavity}}$ , can exceed 20,000. For a 20 cm long sample cell, the effective path length is 8 km. A good CRDS system can achieve a ring-down-to-ring-down variation of 0.03%, leading to a MDAL of  $3 \times 10^{-10} \text{ cm}^{-1}$  ( $0.03 \text{ Mm}^{-1}$ ). For an optical beam diameter of 200 microns, this should be sufficient to detect the optical loss caused by particles as small as 100 nm in diameter. Note also that the CRDS measurement is not dependent on either the intensity fluctuations of the light source, or on the physical sample path length as with traditional absorption spectroscopy.

## 2.2 Concurrent fluorescence detection

Ideal CRDS laser sources are continuous wave (CW) and have narrow linewidths in order to achieve high spectral resolution. These CW lasers can build up significant intracavity powers inside the ring-down cavity and be used for fluorescence detection. The intracavity power can be estimated by the equation:

$$I_{\text{intracavity}} = \frac{P_c T \xi}{1 - R} \quad (4)$$

where  $P_c$  is the power coupled into the cavity mode being observed,  $\xi$  is the injection efficiency (which is a function of cavity length, of laser frequency scanning rate, and its linewidth [16]), and  $T$  and  $R$  are the cavity mirror transmission and reflection coefficients. A four-mirror ring cavity with the roundtrip length of 82 cm with  $R=99.995\%$  ( $1-R = 50 \text{ ppm}$ ) and  $T = 30 \text{ ppm}$ , would have a cavity resonance width of 5.7 kHz, a ring-down time of 14  $\mu\text{s}$ , a free spectral range (FSR) of 357 MHz, and an enhancement factor of about 3,000. If the laser linewidth is negligibly small, and the laser frequency sweep rate corresponds to scanning through 1.5 FSR at a 100 Hz repetition rate, then the normalized frequency scanning speed  $\eta$  will be 6.6, and we can estimate the injection efficiency  $\xi$  to be 0.17 using reference [16]. For a typical CW laser that produces 20 mW of power at 488 nm (a good wavelength for fluorescent microspheres used to generate an aerosol) the intracavity power generated could be as high as 9 watts. Given a TEM<sub>00</sub> mode size of 0.25 mm, the intracavity power density will be on the order of 4 kW/cm<sup>2</sup>. The incident power captured by a 1  $\mu\text{m}$  diameter particle will be approximately 34  $\mu\text{W}$ . For a 1- $\mu\text{m}$ -diameter fluorescein-coated polystyrene sphere, assuming a molar extinction coefficient of 90,000 M<sup>-1</sup>cm<sup>-1</sup>, a single particle will absorb approximately 30% of the incident light. With the intracavity power estimated above, and 50% fluorescence efficiency, this will lead to the generation of approximately 5  $\mu\text{W}$  of fluorescence emission per particle.

To determine the amount of light that will be captured by a fluorescence detector, we need to calculate the amount of emitted fluorescence that can be collected. Consider the case when only one particle is present in the viewing volume. With a system viewing angle of 6 degrees ( $\text{NA}=0.11$ ), the corresponding solid angle is,

$$\Omega = 4\pi \sin^2\left(\frac{\theta}{4}\right) \quad (5)$$

which is  $\Omega=8.6 \times 10^{-3}$  steradians. The fraction of power collected by the optical system will be  $\Omega/4\pi$  ( $7 \times 10^{-4}$ ). Thus, the total power incident onto the detector will be approximately 0.7 nW. A typical photo-multiplier tube (PMT) has a 80 mA/W sensitivity, a  $1 \times 10^6$  gain, and a 20 k $\Omega$  load resistance. Such a PMT produces approximately 6 V of signal per particle. The voltage noise of the PMT under these conditions is expected to be less than 1 mV, which will result in a high S/N ratio.

For a laser whose linewidth exceeds the cavity mode linewidth, the intracavity power will be reduced by the ratio of the respective linewidths. In addition, the laser-frequency scanning

speed will also reduce the intracavity power [16]. Such a reduction factor could easily decrease the enhancement factor by an order of magnitude or more and reduce the single particle S/N ratio accordingly. Nonetheless, such a system should still have the capability of measuring the fluorescence emission from a single particle.

### 3. Experimental section

The CRDS system used in this study is illustrated in Fig. 1. It was comprised of a 488 nm laser, a mode-matching telescope, a ring-down cavity, a ring-down detector, and the two fluorescence detectors. These components are described in greater detail in this section.

#### 3.1 488 nm excitation laser

A Picarro Cyan laser that produces 20 mW of 488 nm light was chosen. This is a highly reliable, single longitudinal mode solid-state laser, which is ideally suited for cavity ring-down applications. The 488 nm wavelength was chosen because it is an appropriate excitation wavelength for many common fluorophores.

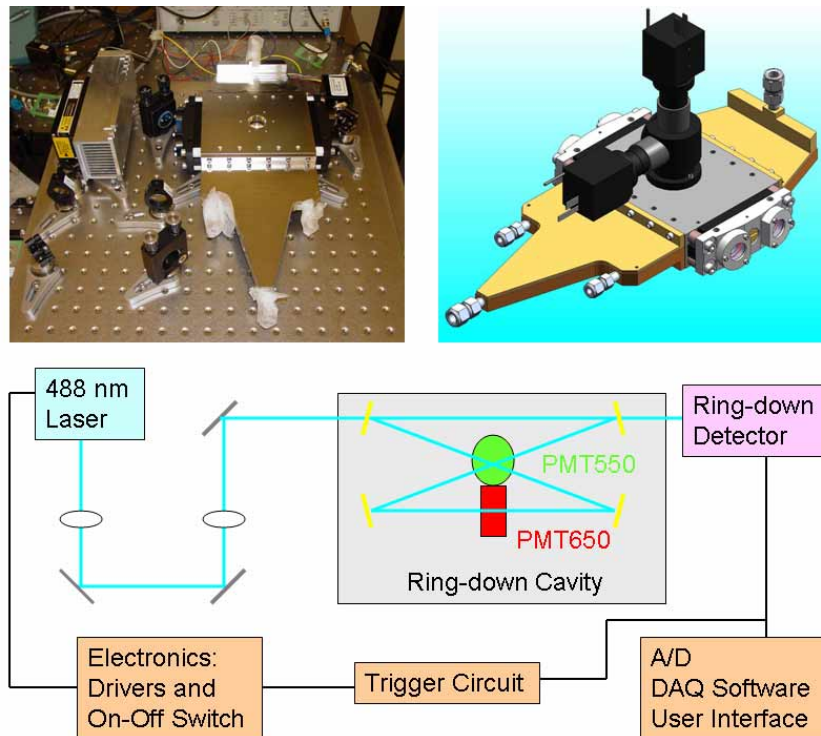


Fig. 1. (Bottom) Cavity ring-down system used for simultaneous measurement of extinction and fluorescence of aerosols. (Top left): photograph of system, (Top right): rendering of the ring-down cavity with fluorescence detection optics attached.

We swept the laser frequency to match the cavity resonance instead of using a piezoelectric transducer (PZT) to dither the optical cavity length. The cavity resonances were very closely spaced in the 82-cm round-trip ring-down cavity, approximately  $0.01 \text{ cm}^{-1}$ , thus requiring only small sweeps in laser wavelength. Also, the cavity mode spacing is insignificant compared to the absorption bandwidths of the fluorophores, which are 100 to  $1000 \text{ cm}^{-1}$ . We modified a standard Cyan laser by applying a purely electronic scheme for sweeping the laser wavelength, and for switching off the laser drive current when the transmitted signal reached a threshold. A ring-down signal was acquired after the laser was switched off, and then the laser was switched back on. When the laser restarted, its

wavelength swept across several cavity resonances. Ideally, the transmitted signal reached threshold again on one of these resonances and the switching cycle was repeated. We included a time-out circuit in the laser switching electronics which was activated if the cavity transmission signal did not reach a threshold value within a certain time, both of which were adjustable parameters. The time-out sequence shut off the laser and restarted it without generating a trigger signal for the data acquisition. This circuit enabled us to acquire ring-down data rapidly and without interruption. A similar scheme was implemented in a measurement system for liquid measurements using CRDS [17].

### 3.2 Ring-down cavity

The ring-down cavity was based on a design similar to that used in earlier aerosol measurement work [7]. The cavity was of a bowtie design consisting of a monolithic resonator made from four identical mirrors with 1 m radius of curvature. This configuration has several advantages, as compared with two- and three-mirror designs, including (i) simplified alignment, (ii) longer optical interaction length for a similar size, and (iii) uniformity of mirror optics.

We specified the cavity mirror coatings to have a total loss of 50-70 ppm ( $R=99.993\%$  to  $99.995\%$ ), and 200-mm mirror separation in the bowtie cavity. This reflectivity was chosen to produce a ring-down time between 10 and 14  $\mu\text{s}$  in the empty cavity. The mirror transmission was expected to be 30 to 50 ppm, and the ideal pump enhancement factor (assuming a perfectly monochromatic pump) 3,000 for the empty cavity, as described above. The aerosol-laden cavity was expected to have a ring-down time approximately 1  $\mu\text{s}$  shorter than the empty cavity and an enhancement factor of 2,400. The actual enhancement factor was reduced by the ratio of the line-width of the excitation laser and the ring-down cavity mode, and the laser frequency sweep rate.

### 3.3 Aerosol generation and gas handling system

The sample flow cell, illustrated in Fig. 2(a), was intended to create a laminar flow perpendicular to the ring-down optical axis [7]. Clean mirror purge flows were also employed to keep the aerosol-laden sample flow from impinging upon and contaminating the cavity mirrors. As part of the work described in [7], a test on a similar flow cell showed that the flow was laminar to the extent that the sample gas did not mix with the purge gas and hence come into contact with the cavity mirrors.

Figure 2(b) is a schematic of the gas handling system surrounding the ring-down cavity. The aerosol generator consisted of an atomizer in which a small flow of dry nitrogen sprayed the microsphere liquid suspension diluted in distilled water. The resulting wet aerosol was then diluted with dried room air to obtain the desired aerosol concentration and to dry the microspheres. The dry-air flow was 6 liters per minute and the pressure was nominally atmospheric. The flow through the ring-down cavity was approximately 3 liters per minute (l/min), 1 l/min of which is sample flow, and 2 l/min of which is purge flow to protect the mirrors. The residence time of the gas in the cavity was calculated to be approximately 3 seconds, and the time of flight across the optical beam was only 10 msec. The time spent within the optical beam is much longer than the measurement time of each ring-down event, but much less than the interval between ring-down events. The remaining  $\sim 5$  l/min of the aerosol flow exited through a shunt to the exhaust. Valves near the cavity inlet controlled the source of the sample gas: either from the aerosol generator or from the "zero air" particle filter. A commercial particle counter designed to monitor clean rooms measured the aerosol concentration.

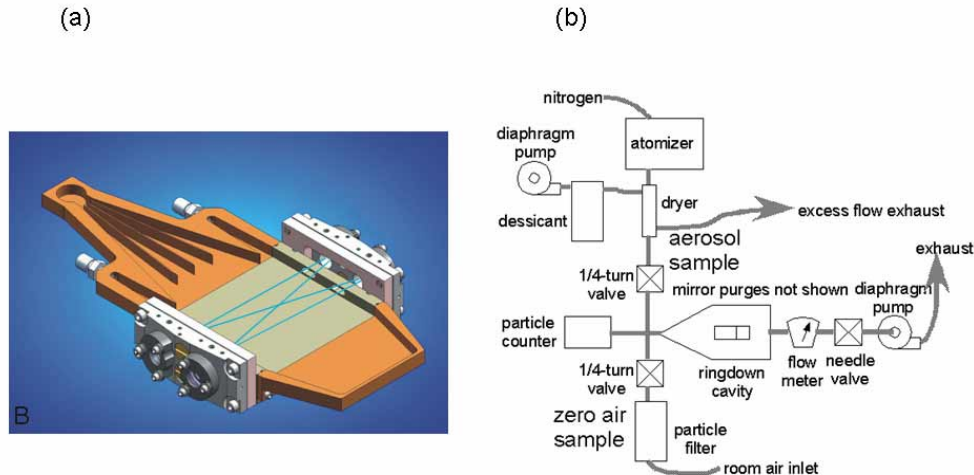


Fig. 2. (a) Cutaway view inside ring-down cavity showing the optical path and (b) gas handling system for ring-down system.

### 3.4 Ring-down detection

An avalanche photodiode monitored the beam transmitted through the ring-down cavity, and its signal was acquired by a computer digitizer and fit to an exponential to characterize the ring-down time of the cavity. The digitized cavity transmission signal was also used to normalize the fluorescence signals.

### 3.5 Fluorescent particles

For fluorescent aerosol, we used T-8880 and T-8883 FluoSpheres (Molecular Probes, Inc., [www.probes.com](http://www.probes.com)) that are specifically designed for 488 nm excitation. These microspheres are unique in that they offer several different emission frequencies for the same excitation frequency (488 nm). The T-8880 FluoSphere has an emission peak at 550 nm wavelength, while the T-8883 FluoSphere has an emission peak at 650 nm.

### 3.6 Fluorescence detection

We designed the optical train and chose optical filters and detectors for the collection of fluorescence from the aerosols. We used photo-multiplier tubes (PMTs) (model H6780-02 from Hamamatsu) to measure the fluorescence signals. The fluorescence detection optics were located in a tower on top of the ring-down cavity, as shown in Fig. 1. The window separating the flow cell from the tower was a long-pass optical filter which transmitted >95% at 550 nm, >99% at 650 nm, and <0.001% at 488 nm wavelengths. An additional optical bandpass filter preceded each PMT. One filter transmitted a wavelength range of 70 nm centered on 550 nm, and the other filter transmitted a range of 70 nm centered on 650 nm. The optical magnification factor was equal to one in each channel, and the numerical aperture was 0.34. We set the gain of the PMTs to their maximum value, at which point their output signal currents occasionally approached the maximum current stated in their specification. With no fluorescent microspheres in the cavity, there were few enough photons incident on these detectors that we could easily distinguish individual photons with the laser off or on.

### 3.7 Data acquisition

A data acquisition computer containing a Gage fast digitizer (model 12100) was chosen for ease of operation. The acquired data for each of the three optical detection channels consisted of the detector voltage as a function of time for fixed periods before and after the trigger signal. The period after the trigger was long enough to capture the entire ring-down event and

a substantial interval after the ring-down had decayed into the detector noise but before the laser restarted. This last interval was used during the data analysis to determine the baseline offset of each detection channel, including both electronic and optical contributions. In the next step of analysis, the signals of each channel were integrated over a selectable time interval in each ring-down event (not including the baseline interval). The inclusion of pre-trigger data in this time interval increased the amount of data (the cavity fills and unfills during this time, but the transmitted signal does not reach threshold), in order to improve the measurement statistics over using only the exponential portion of the ring-down event.

## 4. Results and discussion

### 4.1 CRDS performance

The mode-matching telescope focusing and beam steering was designed and experimentally optimized to minimize excitation of ring-down cavity modes other than TEM<sub>00</sub>, by observing the profile of the beam transmitted through the cavity. The extinction (ratio of TEM<sub>00</sub> excitation to any other mode excitation) was approximately 15 to 20 dB. This extinction was adequate to guarantee triggering the electronics and data acquisition only on TEM<sub>00</sub> excitations.

The average measured ring-down time was initially 9.7 microseconds with 0.3% standard deviation at a data rate of 40 Hz, indicating a mirror reflectivity of 99.993%, a laser cavity mode width of 8 kHz, and a detection limit for the aerosol extinction coefficient of  $6 \times 10^{-9} \text{ cm}^{-1} \text{ Hz}^{-1/2}$ .

Figure 3 shows cavity ring-down time with still, ambient laboratory air in the cavity. There are small drifts in the ring-down time, caused by small changes in the ring-down cavity length, or which longitudinal mode is excited (i.e., the laser wavelength) and the presence of narrow atmospheric absorption lines, such as of water vapor. These variations contribute to the 0.3% standard deviation. The ring-down intensity was monitored as a reference for fluorescence detection.

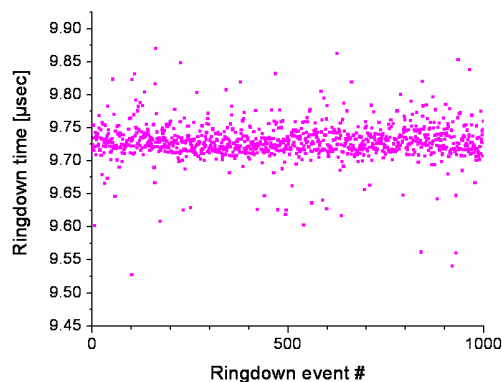


Fig. 3. Measured ring-down time in air over 1000 events (ring-downs).

The ideal cavity enhancement factor corresponding to the 9.7- $\mu$ sec ring-down time, and the total cavity optical path length (820 mm), for a perfectly monochromatic laser is approximately 2500. However, the laser frequency sweep rate during its start-up is a nonlinear function of time, and the corresponding normalized frequency scanning speed  $\eta$  is actually in the range of 10 to 100. This reduces the cavity enhancement factor to a range between 325 and 46. The laser linewidth was estimated to be 1 MHz, which is 60 times larger than the ring-down cavity mode width. In steady state (without the laser frequency sweep), this factor alone would reduce the enhancement factor from 2500 to about 40. The cavity enhancement factor (power circulating inside the cavity divided by the incident power)

calculated from the measured cavity transmission was measured to be approximately 20, which is consistent with contributions from the sweep rate and the large laser linewidth.

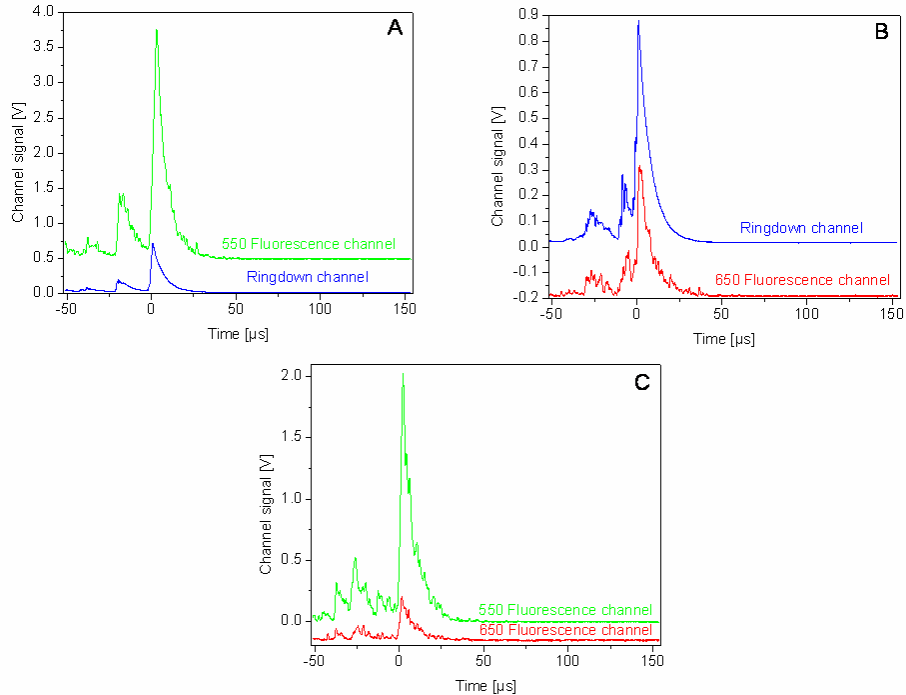


Fig. 4. Comparison between: (a) 550 nm fluorescence channel and ring-down detector, (b) 650 nm fluorescence channel and ring-down detector, and (c) 550 nm and 650 nm channels.

#### 4.2 Fluorescence performance

The detection signals are identified as the 550 channel, the 650 channel, and the RD (ring-down) channel. All possible pairs of these 3 channels were acquired: RD + 550, RD + 650, and 550 + 650. We did not acquire all 3 channels simultaneously because of a lack of compatible multi-channel data acquisition electronics and associated software drivers. However, the pairing provided sufficient data to determine all of the correlations among the signals required to characterize the detection system.

The digitized optical signals were integrated over a selected time interval. These integrals can then be correlated among channels. Figure 4 shows examples of each of the 3 pairs of signal acquisitions comparing the signals within each pair. The trigger occurs at time = 0. Each trace shows the time dependence of a single ring-down event for which significant fluorescence was observed. At the aerosol concentrations used in these experiments, significant fluorescence was observed during most, but not all ring-down events.

Figure 4(a) shows the correlation between the 550 channel and the RD channel with an aerosol of 550 nm fluorescent microspheres (MicroProbe Fluosphere T-8880). Figure 4(b) shows the correlation between the 650 channel and the RD channel with an aerosol of 650 nm fluorescent microspheres (MicroProbe Fluosphere T-8883). To quantify the fluorescence response, the time-integrated fluorescence signals are normalized to the time-integrated RD signals. This normalization is necessary since the cavity fills with different intensities of the excitation laser on each ring-down event, although the ring-down time remains approximately constant.

The fluorescence spectrum of each type of microsphere is broad and will excite both fluorescence detection channels, but by different amounts, based on the spectral overlap of the fluorophore emission and the detection filter transmission characteristics. Therefore, the signal of each channel does not correspond directly to the concentration of the microsphere with its fluorescence peak at that channel. Instead, the microsphere concentrations and fluorescence signals are related to each other by a multi-dimensional linear relation, two-dimensional for our two fluorescent microspheres and two detection channels. The relation can be represented by a 2x2 matrix. The diagonal terms represent the response of each channel to its like microsphere. The off-diagonal terms represent the response of each channel to the other type of microsphere.

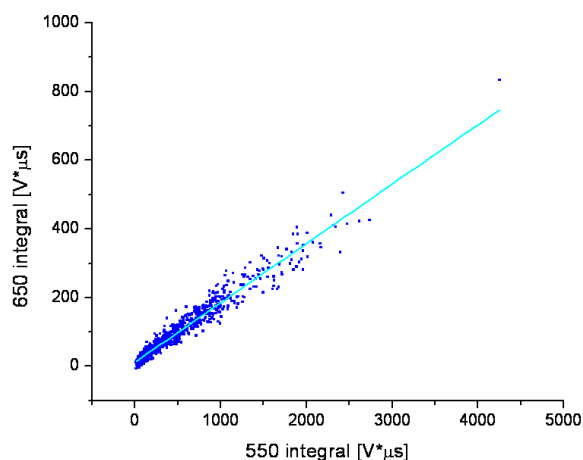


Fig. 5. Correlation between integrated fluorescence signals from the 550 nm and 650 nm fluorescence detectors when using the 550 nm microspheres.

To determine the off-diagonal terms, the fluorescence channel signals are correlated with each other by computing the correlation function and linear regression between their respective integrals in a set of ring-down events. In this manner, the cross-response between the channels can be quantified: the response of the 550 channel to the 650 microspheres, and the response of the 650 channel to the 550 microspheres. Figure 4(c) shows the correlation between the 650 channel and the 550 channel with an aerosol of 550 nm fluorescent microspheres. Figure 5 shows the correlation between the integrated fluorescence signals with the 550 nm microspheres. The linear least-square fit (cyan line in Fig. 5) indicates that the 650 channel responds with an amplitude equal to  $0.168 \pm 0.005$  of the 550 channel signal. This cross-response inherently includes the effects of PMT gain, PMT wavelength response, and optical transmission in each wavelength band from the ring-down cavity to the PMTs. A similar measurement with 650 nm microspheres shows that the 550 channel responds with an amplitude equal to  $0.034 \pm 0.001$  of the 650 channel signal.

The normalized integrated fluorescence of a single microsphere can be estimated from the average fluorescence signal, the independently measured microsphere concentration, the volume of excitation beam observed by the fluorescence detectors, and the sensitivity of the detection. The observed excited volume was approximately  $2.5 \text{ mm}^3$  (0.2 mm excitation beam radius and 20 mm of beam length within the collection volume of the fluorescence detectors). The average 550-channel normalized integrated signal was 0.7 to 0.9 with a 550-microsphere concentration of  $2 \times 10^5$ /liter. Therefore, the 550 channel response is  $\sim 1.6$  per 550-microsphere, i.e. the ratio of the integrated 550 channel to the integrated RD channel is 1.6. The average 650-channel normalized integrated signal was 0.2 to 0.3 with a 650-

microsphere concentration of  $2 \times 10^5$ /liter. Therefore, the 650 channel response is  $\sim 0.5$  per 650-microsphere. The diagonal terms of the matrix are the reciprocals of these values.

To determine the concentrations of the two fluorescent microspheres, the diagonal terms of the matrix are as calculated above. The off-diagonal terms equal the negatives of the cross-responses multiplied by the respective diagonal term:

$$\begin{bmatrix} 550 \text{ spheres} \\ 650 \text{ spheres} \end{bmatrix} = \begin{bmatrix} 0.7 & -0.024 \\ -0.336 & 2 \end{bmatrix} \begin{bmatrix} 550 \text{ channel} \\ 650 \text{ channel} \end{bmatrix} \quad (6)$$

In this equation, the left-hand side represents the number of each microsphere in the observed excited volume, and the column matrix on the right-hand side represents the integrated, normalized fluorescence signals. The 2x2 matrix elements depend on the relative sensitivities of the fluorescence and ring-down detectors, the fluorescence collection efficiency, and the fluorescence strengths of the two types of microspheres. The matrix elements are, in theory, independent of the excitation power, the cavity enhancement factor, and the integration interval. To demonstrate the utility of the matrix equation, we acquired data using a mixture of both types of microsphere. The average normalized integrated 550 channel was 1.15. The average normalized integrated 650 channel was 0.55. Therefore, the average number of 550 microspheres in the observed volume predicted by the matrix equation was 0.8, and the predicted number of 650 microspheres was 0.7. These values correspond to concentrations of  $3.2 \times 10^5$ /liter and  $2.8 \times 10^5$ /liter, respectively.

A measurement using zero air produced a slope dependence of  $< 0.1\%$  of the fluorescence channel signals on the RD channel. The correlations were  $\leq 0.03$ , which is very small, indicating that the dependence is practically insignificant. The correlation and slope were small enough that they may be ignored in the presence of moderate microsphere concentration.

Another measurement using blank microspheres produced a small but significant signal in each fluorescence channel, proportional to the RD channel, and presumably also proportional to the microsphere concentration:  $0.0095 \pm 0.001$  for the 550 channel and  $0.0065 \pm 0.001$  for the 650 channel, both at a concentration of  $2 \times 10^5$  blank microspheres / liter. The correlations were  $< 0.1\%$ , hence the dependence is only slightly significant. This blank response should be subtracted from the fluorescence channels before calculating the concentration of fluorescent microspheres based on the fluorescence signals. However, for the concentrations of fluorescent microspheres used, the blank response was a small fraction of the total fluorescence signals, and was of the same order as the uncertainty of the measurement in the presence of fluorescent microspheres.

The absolute fluorescence of a single microsphere can be estimated similarly as with the normalized fluorescence, but using the signal voltage at the time of trigger (usually the peak signal) instead of the normalized integral. The average 550-channel signal was 0.3 to 0.5 V with a 550-microsphere concentration of  $2 \times 10^5$ /liter. The PMT sensitivity at 550 nm is approximately  $10^5$  A/W, its load resistance was 20 k $\Omega$ , and the transmission to the detector was approximately 0.4. Therefore, the average signal per microsphere is 0.6 to 1 V, which corresponds to 1 nW of collected fluorescence. This is the total light within the  $\sim 50$ -nm-wide fluorescence peak, so the average spectral power is  $\sim 20$  pW/nm. Given that our cavity enhancement factor is only 20, and we assumed 450 in calculating the expected fluorescence collection, we anticipated only 50 pW of collected fluorescence, much less than the observed fluorescence. But we did not know the strength of the fluorescence of individual microspheres, and apparently our estimate of this strength was much too low.

The average 650-channel signal was 0.1 to 0.15 V with a 650-microsphere concentration of  $2 \times 10^5$ /liter. The PMT sensitivity at 650 nm is approximately  $0.5 \times 10^5$  A/W, its load resistance was 20 k $\Omega$ , and the transmission to the detector was approximately 0.4. Therefore, the average signal per microsphere is 0.2 to 0.3 V, corresponding to 0.5 nW of collected fluorescence. This is the total light within the  $\sim 50$ -nm-wide fluorescence peak, so the average spectral power is  $\sim 10$  pW/nm. The fluorescence spectral power integrated over the 10- $\mu$ s

ring-down time is equivalent to several hundred photons per nm. Adding to the signal integration interval the time before the trigger during which the ring-down cavity is filling with the excitation beam will increase this result.

## **5. Concluding remarks**

In summary, we designed a CRDS instrument that could simultaneously measure the absorption loss and fluorescence emission from an aerosol consisting of fluorescently-labelled microspheres. The fluorescence spectral power collected from a single fluorescent microsphere via excitation laser cavity enhancement was measured to be 10 to 20 pW/nm. We expect this power to be sufficient to obtain the spectrum of a single microsphere with a resolution of 10 nm and signal-to-noise ratio of  $\sim 10$ . The relative concentrations of two different types of fluorescent microspheres were determined from a time-integrated fluorescence measurement of a mixture of both.

In the geometry we used, the fluorescence was collected from only a portion of the optical beam path within the ring-down cavity. As a result, the fluorescence was not collected from all of the aerosol particles which affected the ring-down time. One possible improvement to the geometry is to make the ring-down cavity very short, so that the fluorescence can be collected from its entire volume.

Once available, CW lasers emitting in the UV could be employed to access the natural fluorescence emission of bio-aerosols. If CW lasers that concurrently emit harmonics could be developed (e.g., 976 nm and 488 nm and 244 nm), they could be injected into cavities whose mirror coatings exhibit a high reflectivity at all of these harmonics. Simultaneous collection of optical loss, scattering and fluorescence emission spectra could help quantify the physical characteristics of the aerosol (such as albedo or particle size) as well as the composition (biological versus non-biological) of the particulates. Furthermore, such a system would have the potential to leverage non-linear optical spectroscopic processes such as stimulated Raman scattering.

## **Acknowledgments**

We thank Dr. Eric Crosson, Dr. Boris Kharlamov, Dr. Sergei Koulikov, Mr. Hoa Pham, and Mr. Khoi Nguyen for their help in completing this work. This material is based upon work supported by NASA under a Phase I SBIR Grant No. NNA04CB29C.